coatings

MDPI

Article

Photocatalytic Oxidation of Amoxicillin in CPC Reactor over 3D Printed TiO_2-CNT@PETG Static Mixers

Kristina Miklec [1], Ivana Grčić [1,*], Lucija Radetić [1], Ivan Karlo Cingesar [2] and Domagoj Vrsaljko [2]

[1] Faculty of Geotechnical Engineering, University of Zagreb, Hallerova aleja 7, 42000 Varaždin, Croatia
[2] Faculty of Chemical Engineering and Technology, University of Zagreb, Marulićev trg 19, 10000 Zagreb, Croatia
* Correspondence: igrcic@gfv.hr

Abstract: Antibiotics present common pollution in the environment, and they are often found in surface waters. Their presence or decomposition in water under natural sunlight can cause different unwanted consequences on the environment. In this paper, we report the application of 3D printed photocatalysts shaped as helix static mixers for tentative photocatalytic oxidation of antibiotic amoxicillin. The research was carried out in laboratory conditions in a semi-pilot-scale compound parabolic reactor (CPC) with static mixers made from PETG with TiO_2 and MWCNT as fillers. The efficiency of 3D printed photocatalysts was evaluated in terms of amoxicillin decomposition kinetics using a pseudo-first-order kinetic model. The experimental results of amoxicillin decomposition and generated by-products were analyzed by using the Q-TOF LC/MS technique and presented using MassHunter Workstation.

Keywords: amoxicillin; photocatalysis; titanium dioxide (TiO_2 P25); 3D printed static mixers; multiwalled carbon nanotubes (MWCNT); Q-TOF LC/MS

Citation: Miklec, K.; Grčić, I.; Radetić, L.; Cingesar, I.K.; Vrsaljko, D. Photocatalytic Oxidation of Amoxicillin in CPC Reactor over 3D Printed TiO_2-CNT@PETG Static Mixers. *Coatings* **2023**, *13*, 386. https://doi.org/10.3390/coatings13020386

Academic Editor: Emerson Coy

Received: 7 January 2023
Revised: 2 February 2023
Accepted: 6 February 2023
Published: 8 February 2023

1. Introduction

Antibiotics represent one of the main discoveries of the last century that changed the treatment of a large array of infections in a significant way. However, trace levels of pharmaceuticals and their related metabolites are often found in surface waters due to their wide consumption and release through wastewater from households, pharmaceutical industry, hospitals, landfills and run-off from animal feeding operations [1–5]. Antibiotics are found at low concentrations, ng/L to µg/L, which makes them difficult to detect, analyze and degrade at current wastewater treatment plants [6]. The occurrence of antibiotics in municipal wastewater and their distribution in surface waters have been critically discussed in relation to the development and spreading of antibiotic resistance in the environment [7]. In this respect, profound knowledge on the fate of antibiotics in wastewater treatment plants (WWTPs) as well as on their long-term behavior and their TPs in the environment is of importance [8].

Antibiotic residues are difficult to degrade, and even though it has already been known for more than a decade that conventional wastewater treatment methods are not designed for their proper treatment, it is still a major vexing issue. Therefore, it is particularly important to continuously identify, monitor and control the release of pharmaceutical substances into the environment [9,10]. There are several conventional treatment methods for several antibiotic types such as oxidation, filtration, adsorption and combined systems. Unfortunately, due to the lack of proper treatment with suitable efficiency, the occurrence of toxic by-products and high operational costs, alternative new methods are needed today [11,12]. Photocatalytic methods are among the methods that are usually recommended for the treatment of these pollutants [13].

Currently, the emphasis on antibiotics and alternative treatment technologies is even more highlighted due to the COVID-19 pandemic and increased pharmaceuticals consump-

tion in healthcare systems. Therefore, in this paper, an application of the photocatalytic oxidation process for the degradation of residual antibiotic amoxicillin as a model pollutant in accordance with the second Watch list [14] (Table 1) is presented. Amoxicillin is selected as a widely used penicillin-type antibiotic whose presence in the environment has been widely investigated; it is abundant in natural waters despite its rapid hydrolysis and abiotic transformations into various decomposition products (DPs) [15,16].

Table 1. Antibiotics listed on the second Watch list, their maximum acceptable detection limit and monitoring results in Croatia [14].

Substances	Maximum Acceptable Detection Limit	Monitoring Results of Substances
	(μg/L)	(μg/L)
Erythromycin	0.19	<0.00323
Clarithromycin	0.19	<0.00259–<0.00931
Azithromycin	0.19	<0.00309–<0.00623
Amoxicillin	0.078	<0.00442–0.004729
Ciprofloxacin	0.089	0.0345925–0.1416513

Titanium dioxide (TiO_2) photocatalysis is listed as the best available technique (BAT) in the reference document for common wastewater and waste gas treatment/management systems in the chemical sector [17]. TiO_2 has been intensively studied as a heterogeneous photocatalyst and has demonstrated its potential for the degradation of organic compounds in aqueous systems [18,19]. A major difficulty encountered with this material is the time-consuming and uneconomical recovery of TiO_2 and the necessity for high photocatalyst loadings [11].

The main goal of this work was to estimate the efficiency of novel photocatalytic material, i.e., 3D printed static mixers with different TiO_2 and MWCNT ratios. A commercially available titanium dioxide (TiO_2 P25) and multiwalled carbon nanotubes (MWCNTs, CNTs hereafter) were immobilized in a PETG carrier matrix (helix form of a static mixer) in the process of 3D printing. The study is primarily focused on the understanding of phenomena and occurring processes using novel photocatalytic material. Since 3D printed static mixers with TiO_2 and CNTs as fillers have not been previously reported as potential photocatalysts, more insight was necessary. The study clarifies whether the photocatalytic performance of such material could be unanimously defined or if there is more research needed for the application of similar material for the degradation of emerging pollutants.

By 3D printing, it is relatively easy to modify the model and adapt both the external and internal shape and structure of the object to the application and manufacturing requirements [20]. Additionally, 3D printing offers the possibility of creating highly complex geometries with high quality and accuracy at an affordable price, which is not possible with conventional methods [21–24]. The role of a PETG is to present a good carrier for a catalyst. A good carrier must be chemically and biologically inert, insoluble in water, must have as low an energy gap as possible, must be suitable for chemical activation, must be corrosion resistant and must be economically affordable. Our goal was to investigate the applicability of such material since 3D printed material has a unique surface morphology built by additive technology. Functional filament composites of a PETG polymer matrix with TiO_2 and CNT fillers were effectively prepared. All prepared composites were used to successfully 3D print static mixers using the Zortrax M200 3D printer [25]. Some of the printed static mixers are shown in Figure 1. This shape of the static mixer was chosen to improve the mixing of water and increase the contact of organic pollutants with the photocatalytic TiO_2, which is inside the composite polymer material.

Figure 1. PETG static mixer in Helix form (**left**); Static mixers with different contents of TiO_2/CNTs (**right**).

TiO_2 has ability to break down and destroy many types of organic pollutants, which is presented in many papers. However, photocatalysts in which TiO_2 is encapsulated in the polymer matrix were considered ineffective due to mass transfer limitations and scarcity of active species on the surface of photocatalytic material, which is the issue addressed here. The addition of CNTs was considered, thus resulting in photocatalytic oxidation intensification due to enhanced photon absorption in a wider wavelength range, especially in the visible part of solar spectra. The CNTs act as a good electron acceptor and thereby facilitate the separation of electron–hole pairs to prevent their recombination. The mechanism of photocatalytic activity is described as valence band electrons (e^-) of titanium, excited to the conduction band under visible light irradiation, creating holes (h^+) in the valence band [23]. As the presence of a CNT indicates activation in a wider wavelength range and the enhancement of the catalytic activity of TiO_2, it is considered as an advantage in the usage of CNTs in photocatalytic processes [26,27].

The photocatalytic oxidation was performed in a semi-pilot-scale compound parabolic collector (CPC) reactor, which has been considered as a state-of-the-art photocatalytic reactor. As a simulation of sunlight, a modular panel with full-spectra solar lamps with appropriate UVB and UVA irradiation levels was used. A reactor system can be easily scaled up and installed at the outlet of municipal water treatment plants and industrial wastewater or used as an emerging system for water purification on terrain sites. The experimental results consisted of data of antibiotic amoxicillin decomposition obtained using the quadrupole time-of-flight liquid chromatography/mass spectrometry (Q-TOF LC/MS) technique. Based on the experimental results of amoxicillin decomposition in the CPC reactor over static mixers, several degradation by-products were identified and compared with previously published data obtained in similar research.

2. Materials and Methods

The experiments were performed in laboratory conditions in the CPC reactor (compound parabolic collector, Ru-Ve, Zagreb, Croatia). The tubular reactor (length l = 50 cm, radius R = 1.4 cm) was placed in the compound parabolic mirror and connected to a peristaltic pump (Rotarus Smart 30/Rotarus Smart 100; Rpm = 130 L/min). Osram Ultra-Vitalux 300 W lamps were placed at a height h = 10 cm from the reactor and the irradiated part of the CPC was 12 cm (above the static mixer). Using an Analytik Jena UVX radiometer (Analytik Jena US, Upland, CA, USA), the following values were measured for the two lamps used: L1—UVA = 1342.0 mW/cm^2; UVB = 34.0 mW/cm^2; UVC = 92.5 mW/cm^2. L2—UVA = 1890.0 mW/cm^2; UVB = 44.9 mW/cm^2; UVC = 105.5 mW/cm^2. A static mixer (Figure 1) was used as a carrier of catalyst TiO_2 and CNTs in different percentages (Table 2). The model solution was a sample of antibiotic amoxicillin standard (amoxicillin, 95.0%–102.0% anhydrous basis, Sigma-Aldrich, Burlington, MA, USA) (1 L of the sample) in laboratory glass, which was placed in a cooler (Cooler Julabo 300F, temperature: 15 °C). The complete set-up of the experimentation is shown in Figure S1 (Supplementary Materials). The reaction temperature is a critical factor that should be considered when degrading

organic contaminants [28]; therefore, a cooler was used to keep the reaction temperature constant. The polymer matrix in this study was glycol-modified polyethylene terephthalate (PETG) (Devil Design, Mikolow, Poland). As fillers for the fabrication of functional composite filaments, nano-titanium dioxide, trade name AEROXIDE TiO_2 P25 (Evonik Industries, Essen, Germany), and multi-walled carbon nanotubes (MWCNTs) (Sigma-Aldrich, Burlington, MA, USA) were utilized. A Zortrax M200 3D printer (Zortrax, Olsztyn, Poland) was utilized in this work. Fused filament fabrication (FFF) additive manufacturing technology was used in the printer. The filament for this printer had a diameter of 1.75 mm. The first stage was to create a 3D model of the static mixer with Autodesk Fusion 360 CAD (computer-aided design) software (v2.0) [22], and then 3D print it. During the 3D printing, conditions for the PETG were as follows: temperature range of 235 °C to 238 °C for the nozzle, temperature of 85 °C for the platform and infill density of 60%.

Table 2. Static mixers which were used for experiments of solar photocatalysis.

No. of Experiment	Static Mixer	Content of TiO_2 (%)	Content of CNT (%)
0	No Static Mixer (blank)	0	0
1	Reference Static Mixer	0	0
2	Static Mixer with fillers (PETG)	1.50	0.00
3		1.50	0.25
4		1.50	0.50
5		3.00	0.00
6		3.00	0.25
7		3.00	0.50
8		6.00	0.00
9		6.00	0.25
10		6.00	0.50

Fourier transform infra-red (FTIR) spectroscopy was performed by utilizing the PerkinElmer Spectrum One spectrometer unit (PerkinElmer, Waltham, MA, USA) using the ATR technique in the range of 4000 cm^{-1} to 650 cm^{-1}. The FTIR spectra were scanned for the following materials: PETG, PETG–3T–0.25C composite before 3D printing and PETG–3T–0.25C SM, which denotes the static mixer made from the composites used in photocatalytic experiments, 3TiO_2-0.25C@PETG (Figure S3, Supplementary Materials) and compared with literature data [29,30]. Surface properties were studied by measuring water contact angle with a DataPhysics OCA 20 goniometer (DataPhysics Instruments, Filderstadt, Germany) with a water drop size of 2 µL (Figure S4, Supplementary Materials).

Samples were analyzed by a 6530 Q-TOF LC/MS (Agilent, Santa Clara, CA, USA) (Figure S2, Supplementary Materials) and determined by a MassHunter Workstation (Agilent). As a mobile phase, H_2O + 0.1% formic acid and MeOH + ACN + 0.1% formic acid were used, and the method parameters are listed in Table 3.

Table 3. Q-TOF LC/MS method parameters.

Parameter	Value
Flow	0.5 mL/min
Injection Volume	20 µL
Sheath Gas	400 °C
Flow Rate	12 L/min

Table 3. *Cont.*

Parameter	Value
Capillary Voltage	4 kV
Nebulizer Pressure	60 psi
Drying Gas	5 L/min
Gas Temperature	250 °C
Skimmer Voltage	65 V
Octopole RF peak	750 V
Fragmentor Voltage	90 V
m/z Range	40–950
Resolution	4 GHz

3. Results and Discussion

3.1. Results of Photocatalytic Oxidation of Amoxicillin

Photocatalytic oxidation of amoxicillin was performed in a CPC reactor over PETG 3D printed static mixers with and without added TiO_2 and CNTs as fillers. Figures 2 and 3 show the removal of amoxicillin at an initial concentration of 1 mg/L in the CPC reactor in the presence of TiO_2 and CNTs in different ratios, immobilized on PETG static mixers for up to 120 min of photocatalysis. The kinetics of amoxicillin photocatalytic degradation was evaluated by a pseudo-first-order kinetic model. The decay trend is exponential, following the general equation:

$$C(t) = C(0)\, e^{-kt} \quad (1)$$

where C(t) is the amoxicillin concentration at time t, C(0) is the initial concentration of target pollutant and k (min^{-1}) is an apparent decomposition rate constant.

Based on the collected experimental data and observed kinetic rate constants, it is recognized that the reference static mixer (0TiO_2-0CNT@PETG) has the best results regarding amoxicillin concentration decay. This can be ascribed to photolysis. The photolysis decomposition rate was higher without the reference static mixer than it was with it, regardless of enhanced mixing of the reaction mixture in the CPC tube. The reason underlies the absorption of amoxicillin on the static mixer and simultaneous filtering of incoming irradiation by the PETG material, causing the amoxicillin molecules to be shadowed from the irradiation. The PETG static mixer with the same concentration of CNTs and lower concentration of TiO_2 causes a reduction in decomposition. Additionally, an increase in the TiO_2 concentration causes a slower decay.

For each static mixer, the decomposition rate constant was determined, as shown in the Figure 4.

Photocatalytic oxidation of amoxicillin was assumed over static mixers having TiO_2 in their composition. However, as shown in Figures 2c and 4, amoxicillin decomposition rates were quite similar when only 1.5% TiO_2 was added to a static mixer and there was only a slight decrease from the rate observed for the reference static mixer. This finding suggested a dual mechanism of amoxicillin decomposition, i.e., photolysis in bulk solution and •OH radical-directed decomposition on the photocatalyst surface. Although static mixers with 1.5 % TiO_2 appeared optimal for amoxicillin decomposition, one must notice that the clear explanation of respective photocatalytic performance was masked by dominant ongoing photolysis. Moreover, TiO_2 in the mixer composition absorbs UV irradiation, which can be considered as a filtering effect. In the presence of TiO_2, less irradiation is available for photolytic cleavage of amoxicillin in bulk solution and the overall rate is, therefore, decreased for static mixers with 3 and 6% TiO_2. In Figure 3a, it is shown that more TiO_2 in a mixer resulted in a further decrease in amoxicillin decomposition rates. Photocatalytic decomposition rates are considered low due to the position of TiO_2 in mixers. More specifically, TiO_2 particles are found inside the material, with a negligible portion available on the surface of the photocatalyst. The latter was confirmed by FTIR analysis since there is a lack of a broad band for adsorbed H_2O (between 3600 and 3000 cm^{-1}) typically found in TiO_2 samples as a result of water strongly bound to the surface by hydrogen bonds.

Moreover, contact angles for all samples are quite similar (data not shown), while the surface is expected to be completely hydrophilic if TiO_2 dominates on the surface.

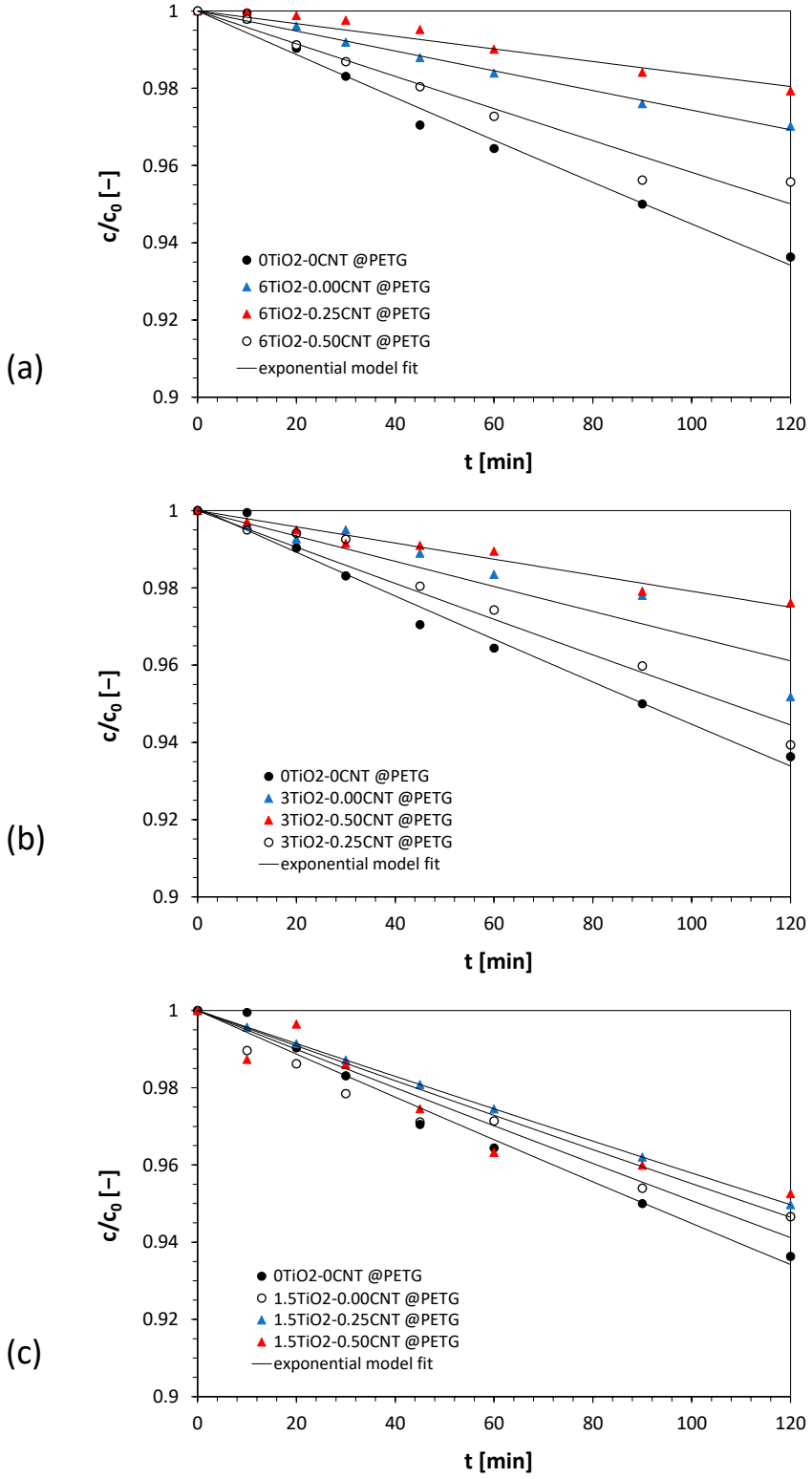

Figure 2. Comparison of observed amoxicillin decomposition trends with static mixers with different concentrations of TiO_2 and CNTs and reference mixer. Kinetics of amoxicillin decomposition using static mixer $6TiO_2$@PETG (**a**), $3TiO_2$@PETG (**b**) and $1.5TiO_2$@PETG (**c**).

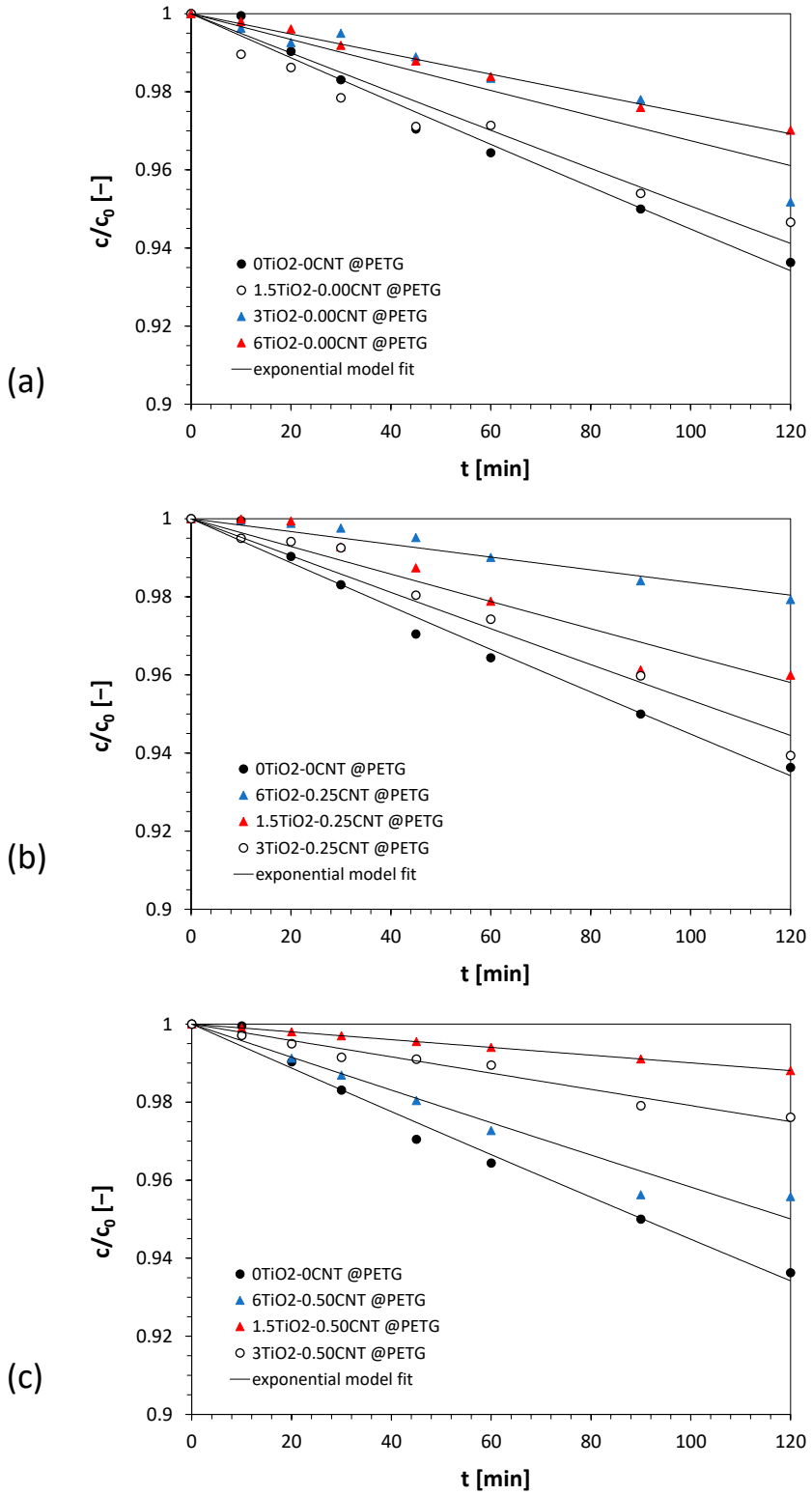

Figure 3. Comparison of observed amoxicillin decomposition trends with static mixers with different concentrations of TiO_2 and CNTs and reference mixer. Kinetics of amoxicillin decomposition using static mixer 0CNT@PETG (**a**), 0.25CNT@PETG (**b**) and 0.50CNT@PETG (**c**).

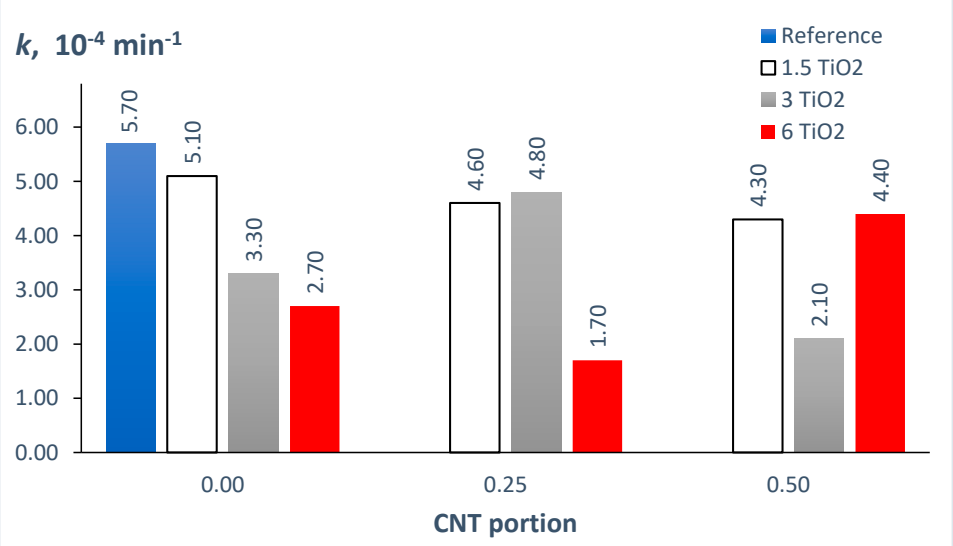

Figure 4. Comparison of amoxicillin decomposition rate constants for different groups of static mixers.

Nevertheless, •OH radicals are formed following TiO_2 excitation due to light absorption. These radicals can migrate to the surface and attack adsorbed amoxicillin molecules. •OH radical-directed amoxicillin decomposition is confirmed by the occurrence of by-products different than those observed during photolysis (reference mixer). The identification of by-products is discussed in the next subsection.

Considering the given explanations, apart from reference and $1.5TiO_2$ static mixers, the highest decomposition rate was observed for the static mixer marked as $3TiO_2$–0.25CNT@PETG. With this particular combination of TiO_2 and CNTs, the parent drug amoxicillin has the highest decrease in concentration in 120 min of photocatalysis and can be considered as the most efficient photocatalyst (Figure 4). Normally, for efficient solar photocatalysis, more CNTs are needed to ensure the capturing of the visible part of incident irradiation. However, in present study, both TiO_2 and CNTs are encapsulated in the photocatalyst formulation and the increase in their respective concentrations did not unbiasedly enhance amoxicillin decomposition rates. In other words, a compromise was necessary to ensure •OH generation and migration to the surface along with enhanced visible light absorption. Similarities in the rates observed for the photocatalysts $3TiO_2$–0.25CNT@PETG and $6TiO_2$–0.5CNT@PETG with similar TiO_2/CNT ratios confirmed the aforementioned statements.

Although a decrease in concentration was achieved, the results could be enhanced if the catalysts were applied directly to the surface of a carrier (PETG static mixer). For future experiments, TiO_2 and CNT should be applied to the surface of a static mixer using an immobilization technique such as dip coating. The reason is that the solar photocatalysis represents a surface phenomenon that is, here, limited to the amount of TiO_2 immobilized and absorbed in PETG carrier in the process of 3D printing.

3.2. Identification of Amoxicillin Degradation Products

The possible amoxicillin degradation products were determined by non-target analysis using the Q-TOF LC/MS technique. As said in a previous work [16], little is known about amoxicillin decomposition and its impact on the environment. Knowing the degradation and transformation pathways of emerging contaminants (ECs) is crucial for several reasons: (i) to assess the risk associated with ECs and their transformation products (TPs) when they reach the environment; (ii) to determine the toxicity of unknown derivatives and (iii) to study processes to promote the removal or the complete degradation of ECs to nonhazardous compounds [31–33]. Furthermore, our results pointed to the highest amoxicillin decomposition rates obtained by photolysis (blank tests). This finding alone

could be used to declare novel 3D printed photocatalysts as ineffective and unworthy of further study. However, it is a well-known fact that photolysis and photocatalysis involve different reaction mechanisms and different by-products may be found. Photolysis alone may result in more toxic by-products, while the photocatalytic reaction pathway involving •OH radicals and other reactive species may help to evade toxic by-products.

As was said in [33], it is well-known that the metabolism of amoxicillin has two major products: amoxicilloic acid and amoxicillin piperazine-2,5-dione (DIKETO). Some minor products were obtained after acid hydrolysis in [34]. To determine the reference degradation products of amoxicillin, samples of model solution were subjected to photolysis experiments under simulated sunlight. The degradation profile was achieved using the Q-TOF LC/MS technique. Moreover, the scientific literature reviewed was used to build a database of amoxicillin decomposition products. The database will be used to investigate the presence of amoxicillin decomposition products in surface waters in Croatia.

Compounds that presented as products of amoxicillin degradation after 120 min of photolysis were determined by target/suspect screening and are shown in Table 4. These compounds were compared to identified by-products after 120 min of photocatalysis in the CPC reactor using $3TiO_2$–0.25CNT@PETG static mixer, which exhibited the highest amoxicillin degradation rate (Table 4).

Table 4. List of compounds determined by MassHunter Workstation and theoretical m/z.

Compound Name	Formula	m/z (exp)	m/z (theo)
Photocatalysis with $3TiO_2$–0.25CNT@PETG static mixer			
Amoxicillin	$C_{16}H_{19}N_3O_5$ S	366.1126	366.1116 [35]
Photocatalysis product #1	$C_{25}H_{38}O_5$	419.2809	419.2809
2-Amino-2-(4-hydroxyphenyl)-N-{(Z)-[3-(4-hydroxyphenyl)-2-oxo-2,3,6,7-tetrahydro1H-1,4-diazepin-5-yl]methylidene}-acetamide	$C_{20}H_{21}N_4O_4$	381.2037	381.1563 [8]
Dehydrocarboxylated amoxicillin penilloic acid	$C_{14}H_{19}N_3O_2NaS$	315.0790	316.1096 [8]
Amoxicillin penicilloic acid	$C_{14}H_{24}N_2O_3S$	301.1427	300 [36]
Photocatalysis product #2	$C_{17}H_{19}N_3$	283.1916	283.1916
Photocatalysis product #3	$C_{10}H_{18}O$	172.1709	172.1709
Photocatalysis product #4	$C_{13}H_{17}NO_4$	249.1603	252.1230 [37]
Photocatalysis product #5	$C_{16}H_{20}N_3O_5S$	369.1725	368 [38]
Photolysis with reference static mixer			
Photolysis product #1	$C_{25}H_{38}O_5$	419.28	419.28
Photolysis product #2	$C_{24}H_{36}O_5$	405.2639	405.2639
Photolysis product #3	$C_{21}H_{29}N_3O$	357.2644	357.244
Photolysis product #4	$C_{14}H_{24}N_2O_7$	350.1905	349 [36]
Photolysis product #5	$C_{12}H_{14}N_4O_3S$	295.0861	295.0861
Photolysis product #6	$C_{17}H_{19}N_3$	283.1906	283.1906
Photolysis product #7	$C_{14}H_{20}N_2O_2$	249.1597	249.1597
Photolysis product #8	$C_{12}H_{11}N$	187.1225	187.1225

The identified compounds after photocatalysis were:

- Amoxicillin (as a parent drug) at a retention time of 6175 min and m/z of 366.1126;
- Photocatalysis product #1 at a retention time of 17,421 min and m/z of 419.2809;
- 2-Amino-2-(4-hydroxyphenyl)-N-{(Z)-[3-(4-hydroxyphenyl)-2-oxo-2,3,6,7-tetrahydro1H-1,4-diaze-pin-5-yl]methylidene}-acetamide at a retention time of 16,969 min and m/z of 381.2037;
- Dehydrocarboxylated amoxicillin penilloic acid at a retention time of 11,898 min and m/z if 315.0790;
- Amoxicillin penicilloic acid at a retention time of 16,617 min and m/z of 301.1427;
- Photocatalysis product #2 at a retention time of 14,910 min and m/z of 283.1916;
- Photocatalysis product #3 at a retention time of 15,161 min and m/z of 172,1709;
- Photocatalysis product #4 at a retention time of 9237 min and m/z of 249.1603;
- Photocatalysis product #5 at a retention time of 12,701 min and m/z of 369.1725.

The identified compounds after photolysis were:

- Photolysis product #1 at a retention time of 17,523 min and m/z of 419.2809;
- Photolysis product #2 at a retention time of 17,172 min and m/z of 405.2639;
- Photolysis product #3 at a retention time of 17,122 min and m/z of 357.2644;
- Photolysis product #4 at a retention time of 9138 min and m/z of 350.1905;
- Photolysis product #5 at a retention time of 13,456 min and m/z of295.0861;
- Photolysis product #6 at a retention time of 14,912 min and m/z of 283.1906;
- Photolysis product #7 at a retention time of 9239 min and m/z of 249.1597;
- Photolysis product #8 at a retention time of 11,800 min and m/z of 187.1225.

The identified degradation by-products from photocatalysis are shown in Figures S5–S30 in Supplementary Materials included in this paper. As can be seen in Figures 5 and 6, there are four by-products (including parent drug amoxicillin) formed during photolysis which are of the same m/z and retention time—as read by a mass spectrometer—as the same by-products formed from photocatalysis. Different by-products formed during the photolysis process are as follows: $C_{24}H_{36}O_5$ (m/z: 405.2639), $C_{21}H_{29}N_3O$ (m/z: 357.2644), $C_{14}H_{24}N_2O_7$ (m/z: 350.1905), $C_{12}H_{14}N_4O_3S$ (m/z: 295.0861) and $C_{12}H_{11}N$ (m/z: 187.1225).

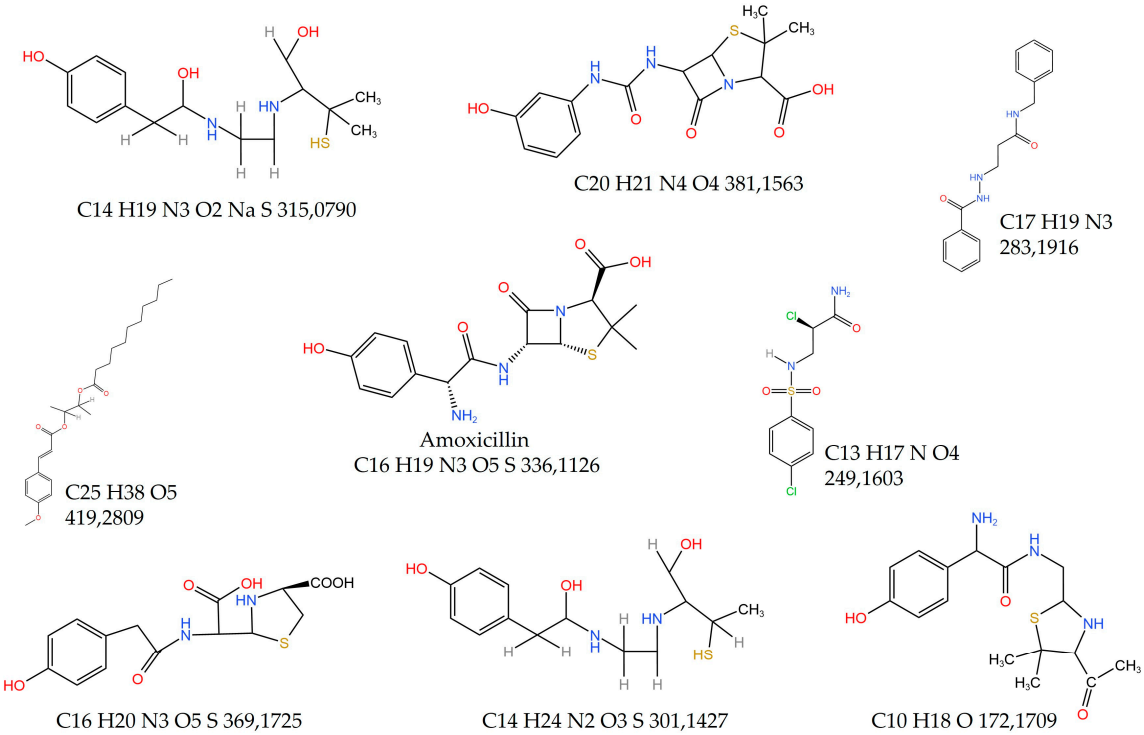

Figure 5. Structures of the identified compounds after 120 min of solar photocatalysis of amoxicillin in CPC reactor over TiO_2–CNT@PETG static mixer.

As can be seen, after both processes, there is a broad range of different by-products. Nevertheless, photolysis of amoxicillin gives one stable polycyclic by-product ($C_{24}H_{36}O_5$ (m/z: 405.2639)), tentatively formed after hydrolysis of the β-lactam ring [39]. Although the amoxicillin decomposition rates calculated based on the decrease in amoxicillin concentration during the photocatalytic process were lower than the calculated rate for photolysis (blank), photocatalysis undergoes a different reaction mechanism, presumably directed by •OH radical formation. The latter resulted in not only hydrolysis of the β-lactam ring, but also hydroxylation of other parts of molecules, bond cleavages and ring openings.

Considering the low availability of photocatalytic active species on the surface of 3D printed static mixers, but also the obvious difference in the composition of organic species after only 120 min of photocatalysis compared to photolysis alone, one can conclude that 3D printed photocatalysts offer a breakthrough in photocatalysis. However, TiO_2 load on the surface should be increased by proper coating procedures.

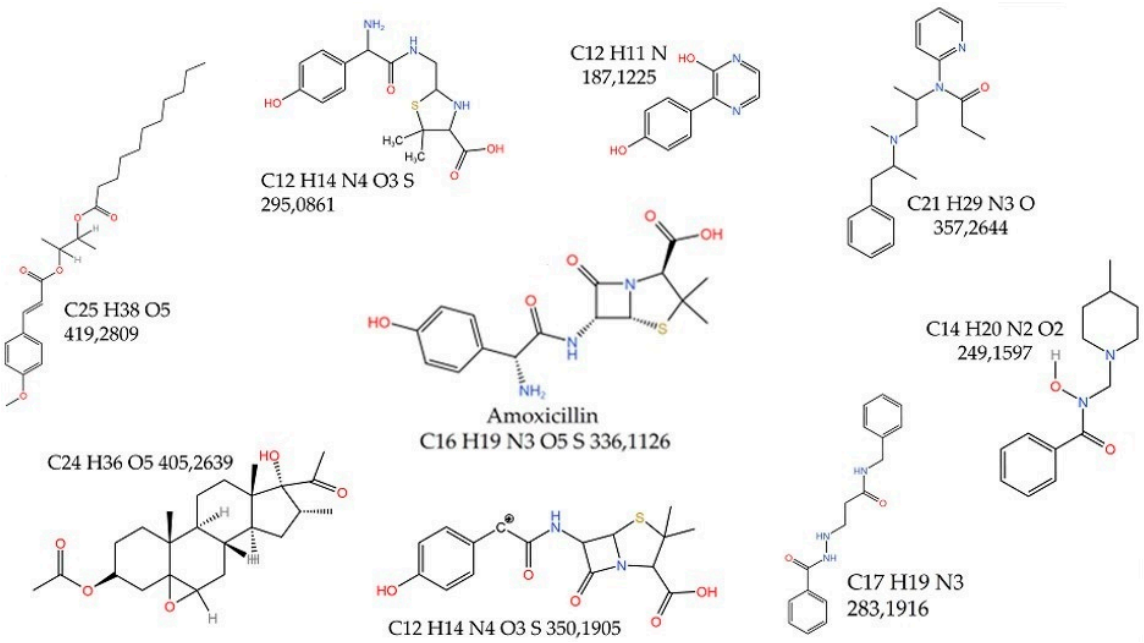

Figure 6. Structures of the identified compounds after 120 min of photolysis.

4. Conclusions

It has been proven by experiments that amoxicillin is a persistent water-borne pollutant and has a broad range of decomposition products. Furthermore, novel 3D printed photocatalysts show activity under the radiation that was used in the experiments. It has been proven that static mixers made of TiO_2–CNT@PETG carriers have good potential for the application of photocatalysis on a larger scale, but it is necessary to coat the surface with additional TiO_2 or another semiconductor material with similar optical properties.

MassHunter software was used for the identification of degradation products of the parent drug amoxicillin. The decomposition products were extracted from the Q-TOF data by target/suspect screening and compounds were filtered out by the Find by Formula algorithm. Finally, thirteen decomposition products were identified by photolysis and photocatalysis. After 120 min of amoxicillin decomposition under artificial solar irradiation, nine different by-products occurred when photocatalytically active 3D printed static mixers were used, while eight by-products were identified for photolysis alone. Evaluation of the by-products gave an insight into reaction pathways.

Based on the results of the experiments, it can be concluded that amoxicillin undergoes decomposition by both photolytic cleavage and photocatalysis when using TiO_2 and CNTs. In this study, amoxicillin degradation by solar photocatalysis was effectively achieved in aqueous solution. With this study, we prove that we can effectively remove organic pollutants (in this case, amoxicillin) with simple and cheap technology. With the addition of carbon nanotubes, an attempt was made to improve the existing photocatalyst to enhance photon absorption in a wider wavelength range. To study the influence of CNTs deeper, future studies should focus on the efficient coating of 3D static mixers on surfaces with both TiO_2 and CNTs and repetition of the experiments in CPC reactors under solar irradiation.

Future experiments will be also based on the research of other organic pollutants from the second Watch list and their degradation products, as well as the modification of the TiO_2/CNT photocatalyst coated on PETG static mixers. The compounds considered to be potential degradation products will be subjected to further analysis.

Supplementary Materials: The following supporting information can be downloaded at: https://www.mdpi.com/article/10.3390/coatings13020386/s1, Figure S1. Experimental system—CPC reactor in Laboratory for Environmental Engineering (Faculty of Geotechnical Engineering, University of Zagreb); Figure S2. Q-TOF LC/MS (Faculty of Geotechnical Engineering, University of Zagreb); Figure S3. FTIR spectra of PETG, PETG–3T–0.25C and PETG–3T–0.25C SM; Figure S4. Visualization of water drop on static mixers with fillers: (from left to right) $3TiO_2$–0CNT@PETG, $3TiO_2$–0.25CNT@PETG, $3TiO_2$–0.5CNT@PETG; Figure S5. Chromatogram results—amoxicillin; Figure S6. MS spectrum results—amoxicillin; Figure S7. Chromatogram results—Photocatalysis product #1; Figure S8. MS spectrum results—Photocatalysis product #1; Figure S9. Chromatogram results—2-Amino-2-(4-hydroxyphenyl)-N-{(Z)-[3-(4-hydroxyphenyl)-2-oxo-2,3,6,7-tetrahydro1H-1,4-diaze-pin-5-yl]methylidene}-acetamide; Figure S10. MS spectrum results—2-Amino-2-(4-hydroxyphenyl)-N-{(Z)-[3-(4-hydroxyphenyl)-2-oxo-2,3,6,7-tetrahydro1H-1,4-diaze-pin-5-yl]methylidene}-acetamide; Figure S11. Chromatogram results—Dehydrocarboxylated amoxicillin penilloic acid; Figure S12. MS spectrum results—Dehydrocarboxylated amoxicillin penilloic acid; Figure S13. Chromatogram results—Amoxicillin penicilloic acid; Figure S14. MS spectrum results—Amoxicillin penicilloic acid; Figure S15. Chromatogram results—Photocatalysis product #2; Figure S16. MS spectrum results—Photocatalysis product #2; Figure S17. Chromatogram results—Photocatalysis product #3; Figure S18. MS spectrum results—Photocatalysis product #3; Figure S19. Chromatogram results—Photocatalysis product #4; Figure S20. MS spectrum results—Photocatalysis product #4; Figure S21. Chromatogram results—Photocatalysis product 5; Figure S22. MS spectrum results—Photocatalysis product #5; Figure S23. Chromatogram and MS spectrum results of photolysis product #1; Figure S24. Chromatogram and MS spectrum results of photolysis product #2; Figure S25. Chromatogram and MS spectrum results of photolysis product #3; Figure S26. Chromatogram and MS spectrum results of photolysis product #4; Figure S27. Chromatogram and MS spectrum results of photolysis product #5; Figure S28. Chromatogram and MS spectrum results of photolysis product #6; Figure S29. Chromatogram and MS spectrum results of photolysis product #7; Figure S30. Chromatogram and MS spectrum results of photolysis product #8.

Author Contributions: All authors contributed to the study's conception and design. Experimentation and analytical method were performed by K.M.; material preparation was performed by I.K.C. and D.V.; data collection and data analysis were performed by K.M., L.R. and I.G. The first draft of the manuscript was performed by K.M., and all authors commented on previous versions of the manuscript. All authors have read and agreed to the published version of the manuscript.

Funding: This research was funded by Waste & Sun for photocatalytic degradation of micropollutants in water (OS-Mi), supported by the European Regional Development Fund, KK.01.1.1.04.0006. and by the Croatian Science Foundation under the project DOK-2020-01-8955.

Institutional Review Board Statement: Not applicable.

Informed Consent Statement: Not applicable.

Data Availability Statement: All the data used to support this study are included within the article.

Conflicts of Interest: The authors declare no conflict of interest.

References

1. Polianciuc, S.I.; Gurzău, A.E.; Kiss, B.; Ştefan, M.G.; Loghin, F. Antibiotics in the environment: Causes and consequences. *Med. Pharm. Rep.* **2020**, *93*, 231–240. [CrossRef] [PubMed]
2. Stefanakis, A.I.; Becker, J.A. A Review of Emerging Contaminants in Water: Classification, Sources, and Potential Risks. In *Impact of Water Pollution on Human Health and Environmental Sustainability*; IGI Global: Hershey, PA, USA, 2016; pp. 55–80. [CrossRef]
3. Nasuhoglu, D.; Rodayan, A.; Berk, D.; Yargeau, V. Removal of the antibiotic levofloxacin (LEVO) in water by ozonation and TiO_2 photocatalysis. *Chem. Eng. J.* **2012**, *189–190*, 41–48. [CrossRef]
4. Elmolla, E.S.; Chaudhuri, M. The feasibility of using combined TiO2 photocatalysis-SBR process for antibiotic wastewater treatment. *Desalination* **2011**, *272*, 218–224. [CrossRef]
5. Luo, Y.; Guo, W.; Ngo, H.H.; Nghiem, L.D.; Hai, F.I.; Zhang, J.; Liang, S.; Wang, X.C. A review on the occurrence of micropollutants in the aquatic environment and their fate and removal during wastewater treatment. *Sci. Total Environ.* **2014**, *473–474*, 619–641. [CrossRef] [PubMed]
6. Demirezen, D.A.; Yıldız, Y.S.; Yılmaz, D.D. Amoxicillin degradation using green synthesized iron oxide nanoparticles: Kinetics and mechanism analysis. *Environ. Nanotechnol. Monit. Manag.* **2019**, *11*, 100219. [CrossRef]

7. Michael, I.; Rizzo, L.; McArdell, C.S.; Manaia, C.M.; Merlin, C.; Schwartz, T.; Dagot, C.; Fatta-Kassinos, D. Urban wastewater treatment plants as hotspots for the release of antibiotics in the environment: A review. *Water Res.* **2013**, *47*, 957–995. [CrossRef]
8. Hirte, K.; Seiwert, B.; Schüürmann, G.; Reemtsma, T. New hydrolysis products of the beta-lactam antibiotic amoxicillin, their pH-dependent formation and search in municipal wastewater. *Water Res.* **2016**, *88*, 880–888. [CrossRef]
9. Wang, J.; Zhuan, R. Degradation of antibiotics by advanced oxidation processes: An overview. *Sci. Total Environ.* **2020**, *701*, 135023. [CrossRef]
10. Baranauskaite-Fedorova, I.; Dvarioniene, J. Management of Macrolide Antibiotics (Erythromycin, Clarithromycin and Azithromycin) in the Environment: A Case Study of Environmental Pollution in Lithuania. *Water* **2023**, *15*, 10. [CrossRef]
11. Gaya, U.I.; Abdullah, A.H. Heterogeneous photocatalytic degradation of organic contaminants over titanium dioxide: A review of fundamentals, progress and problems. *J. Photochem. Photobiol. C Photochem. Rev.* **2008**, *9*, 1–12. [CrossRef]
12. Vasilachi, I.C.; Asiminicesei, D.M.; Fertu, D.I.; Gavrilescu, M. Occurrence and Fate of Emerging Pollutants in Water Environment and Options for Their Removal. *Water* **2021**, *13*, 181. [CrossRef]
13. Iervolino, G.; Zammit, I.; Vaiano, V.; Rizzo, L. Limitations and Prospects for Wastewater Treatment by UV and Visible-Light-Active Heterogeneous Photocatalysis: A Critical Review. *Top. Curr. Chem.* **2019**, *378*, 7. [CrossRef]
14. Hrvatske vode. *Report on Monitoring of Substances from the Second Watch List in Surface Waters of the Republic of Croatia for 2019*; Hrvatske vode (Croatian Waters): Zagreb, Croatia, 2020.
15. Gozlan, I.; Rotstein, A.; Avisar, D. Amoxicillin-degradation products formed under controlled environmental conditions: Identification and determination in the aquatic environment. *Chemosphere* **2013**, *91*, 985–992. [CrossRef]
16. Ellepola, N.; Rubasinghege, G. Heterogeneous Photocatalysis of Amoxicillin under Natural Conditions and High-Intensity Light: Fate, Transformation, and Mineralogical Impacts. *Environments* **2022**, *9*, 77. [CrossRef]
17. Brinkmann, T.; Giner Santonja, G.; Yükseler, H.; Roudier, S.; Delgado Sancho, L. *Best Available Techniques (BAT) Reference Document for Common Waste Water and Waste Gas Treatment/Management Systems in the Chemical Sector*; European Commission: Brussels, Belgium, 2016.
18. Roets, E.; De Pourcq, P.; Toppet, S.; Hoogmartens, J.; Vanderhaeghe, H.; Williams, D.H.; Smith, R.J. Isolation and structure elucidation of ampicillin and amoxicillin oligomers. *J. Chromatogr. A* **1984**, *303*, 117–129. [CrossRef]
19. Kanakaraju, D.; Kockler, J.; Motti, C.A.; Glass, B.D.; Oelgemöller, M. Titanium dioxide/zeolite integrated photocatalytic adsorbents for the degradation of amoxicillin. *Appl. Catal. B Environ.* **2015**, *166–167*, 45–55. [CrossRef]
20. Gibson, I.; Rosen, D.; Stucker, B. *Additive Manufacturing Technologies, 3D Printing, Rapid Prototyping, and Direct Digital Manufacturing*, 2nd ed.; Springer: New York, NY, USA, 2015; pp. 1–374. [CrossRef]
21. Ahmadifar, M.; Benfriha, K.; Shirinbayan, M.; Tcharkhtchi, A. Additive Manufacturing of Polymer-Based Composites Using Fused Filament Fabrication (FFF): A Review. *Appl. Compos. Mater.* **2021**, *28*, 1335–1380. [CrossRef]
22. Liu, Z.; Zhang, M.; Bhandari, B.; Wang, Y. 3D printing: Printing precision and application in food sector. *Trends Food Sci. Technol.* **2017**, *69*, 83–94. [CrossRef]
23. Cuan-Urquizo, E.; Barocio, E.; Tejada-Ortigoza, V.; Pipes, R.B.; Rodriguez, C.A.; Roman-Flores, A. Characterization of the Mechanical Properties of FFF Structures and Materials: A Review on the Experimental, Computational and Theoretical Approaches. *Materials* **2019**, *12*, 895. [CrossRef]
24. Marković, M.-P.; Cingesar, I.K.; Keran, L.; Prlić, D.; Grčić, I.; Vrsaljko, D. Thermal and Mechanical Characterization of the New Functional Composites Used for 3D Printing of Static Mixers. *Materials* **2022**, *15*, 6713. [CrossRef]
25. Karthika, V.; Arumugam, A. Synthesis and characterization of MWCNT/TiO2/Au nanocomposite for photocatalytic and antimicrobial activity. *IET Nanobiotechnol.* **2017**, *11*, 113–118. [CrossRef] [PubMed]
26. Phan, T.L.; Yu, W.J. CVD-Grown Carbon Nanotube Branches on Black Silicon Stems for Ultrahigh Absorbance in Wide Wavelength Range. *Sci. Rep.* **2020**, *10*, 3441. [CrossRef] [PubMed]
27. Duan, Q.; Lee, J.; Liu, Y.; Qi, H. Preparation and Photocatalytic Performance of MWCNTs/TiO2 Nanocomposites for Degradation of Aqueous Substrate. *J. Chem.* **2016**, *2016*, 1262017. [CrossRef]
28. Zhao, J.; Sun, Y.; Wu, F.; Shi, M.; Liu, X. Oxidative Degradation of Amoxicillin in Aqueous Solution by Thermally Activated Persulfate. *J. Chem.* **2019**, *2019*, 2505823. [CrossRef]
29. Latko-Durałek, P.; Dydek, K.; Boczkowska, A. Thermal, Rheological and Mechanical Properties of PETG/rPETG Blends. *J. Polim. Environ.* **2019**, *27*, 2600–2606. [CrossRef]
30. Paszkiewicz, S.; Szymczyk, A.; Pawlikowska, D.; Irska, I.; Taraghi, I.; Pilawka, R.; Gu, J.; Li, X.; Tu, Y.; Piesowicz, E. Synthesis and characterization of poly(ethylene terephthalate-co-1,4-cyclohexanedimethylene terephtlatate)-block-poly(tetramethylene oxide) copolymers. *RSC Adv.* **2017**, *7*, 41745–41754. [CrossRef]
31. Da Silva, A.K.; Amador, J.; Cherchi, C.; Miller, S.M.; Morse, A.N.; Pellegrin, M.-L.; Wells, M.J.M. Emerging pollutants - part I: Occurrence, fate and transport. *Water Environ. Res.* **2013**, *85*, 1978–2021. [CrossRef]
32. Deblonde, T.; Cossu-Leguille, C.; Hartemann, P. Emerging pollutants in wastewater: A review of the literature. *Int. J. Hyg. Environ. Health* **2011**, *214*, 442–448. [CrossRef]
33. Bazzan Arsand, J.; Barcellos Hoff, R.; Jank, L.; Meirelles, L.N.; Diaz-Cruz, M.S.; Mara Pizzolato, T.; Barcelo, D. Transformation products of amoxicillin and ampicillin after photolysis in aqueous matrices: Identification and kinetics. *Sci. Total Environ.* **2018**, *642*, 954–967. [CrossRef]

34. Nägele, E.; Moritz, R. Structure elucidation of degradation products of the antibiotic amoxicillin with ion trap MSn and accurate mass determination by ESI TOF. *J. Am. Soc. Mass Spectrom.* **2005**, *16*, 1670–1676. [CrossRef]
35. Frański, R.; Czerniel, J.; Kowalska, M.; Frańska, M. Electrospray ionization collision induced dissociation tandem mass spectrometry of amoxicillin and ampicillin and their degradation products. *Rapid Commun. Mass Spectrom.* **2014**, *28*, 713–722. [CrossRef]
36. Weng, X.; Cai, W.; Lin, S.; Chen, Z. Degradation mechanism of amoxicillin using clay supported nanoscale zerovalent iron. *Appl. Clay Sci.* **2017**, *147*, 137–142. [CrossRef]
37. Trovó, A.G.; Pupo, N.; Agüera, A.; Fernandez-Alba, A.R.; Malato, S. Degradation of the antibiotic amoxicillin by photo-Fenton process—Chemical and toxicological assessment. *Water Res.* **2011**, *45*, 1394–1402. [CrossRef]
38. Dou, M.; Wang, J.; Gao, B.; Xu, C.; Yang, F. Photocatalytic difference of amoxicillin and cefotaxime under visible light by mesoporous g-C3N4: Mechanism, degradation pathway and DFT calculation. *Chem. Eng. J.* **2020**, *383*, 123–134. [CrossRef]
39. Timm, A.; Borowska, E.; Majewsky, M.; Merel, S.; Zwiener, C.; Bräse, S.; Horn, H. Photolysis of four β-lactam antibiotics under simulated environmental conditions: Degradation, transformation products and antibacterial activity. *Sci. Total Environ.* **2019**, *651*, 1605–1612. [CrossRef]